CIVIL ENGINEERING

Elastoplastic analysis of reinforced concrete space frames using the uniaxial and biaxial bending method

Pedro Cláudio dos Santos Vieira[1]* and **William Taylor Matias Silva[2]**

[1]Centro das Ciências Exatas e das Tecnologias, Universidade Federal do Oeste da Bahia, Rua Professor José Seabra de Lemos, 316, 47805-028, Barreiras, Bahia, Brazil. [2]Departamento de Engenharia Civil e Ambiental, Faculdade de Tecnologia, Universidade de Brasília, Brasília, Distrito Federal, Brazil. *Author for correspondence. Email: pcsvieira@gmail.com

ABSTRACT. The scope of the work involves reinforced concrete frame structures with variations in structural design conception for columns with biaxial bending or uniaxial bending. The beams are designed with simple bending criteria for singly or doubly reinforced beams, or uniaxial bending. The analysis and design criteria are according to NBR 6118:2014. Structure analysis in elastoplastic regimen with the incremental analysis method is performed to detect plastic hinge formation order, collapse load factor, displacements, and rotation capacity of cross sections with the criteria established in the current building codes. The study evaluates the influence of the defined concepts on the structure's elastoplastic behavior. The biaxial and uniaxial bending method is presented as an important formulation for obtaining the collapse load factor using the elastic stiffness matrix with modifications. The algorithms presented enable the development of research without the need for expensive commercial software licenses.

Keywords: analytic method; reinforced concrete; elastoplastic analysis; incremental analysis; design conception.

Introduction

The method of incremental elastoplastic analysis determines the collapse load factor by successive elastic analyses, where for each increment the formation order of the hinges and their respective sections is verified. The appearance of each hinge changes the stiffness of the element, that is, the matrix K will have the same size, but with some altered properties. However, equilibrium matrices L and rotation R are not changed. The stiffness methods of analysis presented, for instance, in Harrison (1973) enable changes to be made without difficulty.

The approach of the present study was designed for reinforced concrete structures and based on the idea proposed by Mello (2003) for uniaxial and biaxial bending but applied according to NBR 6118 (*Associação Brasileira de Normas Técnicas* [ABNT], 2014).

There are many methods for studying the formation process of plastic hinges that use backward algorithms, such as Backward Euler method, and interaction surfaces. (Silva, 2004) performs first-order elastoplastic analysis of steel structures using a predictor/corrector scheme to maintain sectional efforts over an interaction surface that defines the ultimate limit state of the cross section. Vieira and Silva (2013) use multiple linear regression to treat the resultant efforts of several analyses for obtaining a yielding surface with the combined efforts of a space frame analysis. Orbison, McGuire, and Abel (1982) presented 'a model in which material nonlinearity is simulated by the formation of plastic zones of zero length at the ends of the elements. Second order elastic effects are incorporated through a geometrical stiffness matrix. An updated Lagrangian approach is employed'. Their method uses plastic zones of zero length at the ends of the elements too and the 'development of a scheme for controlling the movement of a plastified force point over the yield surface in an approximate but satisfactory manner'.

Barham, Aref, and Dargush (2005) presented 'the derivation and implementation of a flexibility-based large increment method (LIM) for solving nonlinear structural problems. The finite element displacement and force approaches have been developed for solving nonlinear structural problem. The displacement-based finite element method requires a step-by-step approach for material nonlinear analysis that depends on flow theory. Furthermore, significant mesh refinement is often required in plastic zones'.

Inel and Ozmen (2006) explain a method of pushover analysis in which 'the plastic hinge length and transverse reinforcement spacing are assumed to be effective parameters in the user-defined hinge

properties. Observations show that plastic hinge length and transverse reinforcement spacing have no influence on the base shear capacity, while these parameters have considerable effects on the displacement capacity of the frames. Comparisons point out that an increase in the amount of transverse reinforcement improves the displacement capacity'. Patel (2014) and Inel and Ozmen (2006) use the SAP2000 program (Computers & Structures, Inc, 2022). This method is a much simpler process for obtaining plastic hinges and their load factors without the use of reduced stiffness matrix or mesh refinement or plastic hinge length methods as, for example in the processes proposed by Silva (2004), Barham et al. (2005) and Inel and Ozmen (2006).

Salihovic and Ademovic (2017) worked with 'distributed plasticity models or so-called fiber section models, used to simulate the spread of plasticity along the member length and across the section. Fiber hinges are used to define the coupled axial force and bending behavior at locations along the length of a frame element. The cross section is discretized into a series of representative axial fibers which extend longitudinally along the hinge length. These hinges are elastic-plastic and consist of a set of material points, each representing a portion of the frame cross-section having the same material'.

The method is based on the criterion of the Minimum Euclidean norm with property changes of the elastic stiffness matrix. The advantage of this method is that it uses elastic analysis in each phase of the plastic hinge formation process with property changes in the stiffness matrix for space frames without the use of mesh or integration over the cross section generally used in MEF models, as in Salihovic and Ademovic (2017) or Hanganu (1997).

This method introduces a simplicity into the design of perfectly plastic structures which parallels that of the analysis of linear elastic models. This study involves the concepts of structural design, and models of structural dimensioning with theories of singly reinforced or doubly reinforced bending beams, and columns with uniaxial or biaxial bending. The method has proved to be effective in the process of detecting plastic hinges, of obtaining the load factor of the structure's plastic collapse and permitting the choice of a less costly design conception.

Material and methods

The research was developed based on the formulations presented in the sections and on 2 (two) case studies also presented.

Static and elastic analysis

Problem solution in structural mechanics requires the application of three basic sets of laws: Statics, kinematics, and the material's constitutive relations. Two distinct ways can be used to describe such laws, namely, the mesh and the nodal descriptions. Below the relation between them is presented as, for instance, in Harrison (1973).

$$a = L \cdot m; \tag{1a}$$

$$\theta = L^T \cdot \delta \tag{1b}$$

where:
a is the external nodal loads vector; L is the equilibrium matrix of the element; m is the sectional stresses vector; θ represents the cross-section strains associated with the nodal loads vector; and δ is the structure displacements vector.

The equilibrium matrix L is only determined for a structure where no link (internal or external) is violated in its obtention. The same is presented in the formulation of the stiffness methods of analysis used in Harrison (1973).

The method employed in this study was the stiffness method of analysis that uses the member stiffness matrices K, equilibrium L, and rotation R for each unconnected element as in Harrison (1973).

The member stiffness matrix S of the structure is:

$$S = R \cdot L \cdot K \cdot L^T \cdot R^T \tag{2}$$

The stiffness method of analysis was employed because the matrix K is fundamental for the use of the incremental analysis method. The discretization of the continuum in bar elements in the system of local axes (m) follows a formulation based on Harrison (1973).
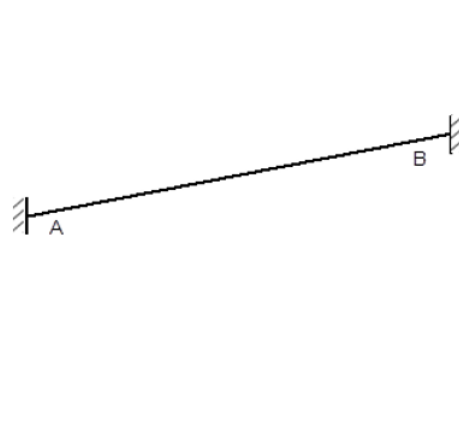
Elastoplastic analysis – incremental method

The method of incremental elastoplastic analysis determines the collapse load factor by successive elastic analysis, where for each increment the formation order of the hinges and their respective sections is verified. The formation of each hinge modifies the stiffness of the element for the proposed method. It means that the matrix K will have the same size, but with some altered elements. Following this method, when the element loses its resistance capacity, the member stiffness matrix K changes Equation 3 (Figure 1) until 6 is in accordance with the hinge formation process.

In this case, the resistance capacity of the axial stiffness is applied as the last value of the section in order that the matrix does not become an identity (I) completely. The equilibrium matrices L and the rotation R remain unchanged. The direct stiffness method of analysis (Harrison, 1973), allows for modifications in the stiffness matrix of the element to be made without difficulty.

The elastoplastic model disregards the curved section relationships of moment and curvature, being elastic until it reaches the plastic moment (M_p), and perfectly plastic for curvature increments (K).

The stiffness matrix K of the unconnected element for the incorporation of hinges, before and during the plastic phase of the structure, has the following possible cases:

Unconnected element with both ends fixed

$$
\begin{bmatrix} T_m \\ MAB_{zm} \\ MBA_{zm} \\ MAB_{ym} \\ MBA_{ym} \\ Q_m \end{bmatrix} =
\begin{bmatrix}
\frac{EA}{L} & 0 & 0 & 0 & 0 & 0 \\
0 & \frac{4EI_z}{L} & \frac{2EI_z}{L} & 0 & 0 & 0 \\
0 & \frac{2EI_z}{L} & \frac{4EI_z}{L} & 0 & 0 & 0 \\
0 & 0 & 0 & \frac{4EI_y}{L} & \frac{2EI_y}{L} & 0 \\
0 & 0 & 0 & \frac{2EI_y}{L} & \frac{4EI_y}{L} & 0 \\
0 & 0 & 0 & 0 & 0 & \frac{GI_x}{L}
\end{bmatrix}
\begin{bmatrix} e \\ \phi AB_z \\ \phi BA_z \\ \phi AB_y \\ \phi BA_y \\ \beta \end{bmatrix} \quad (3)
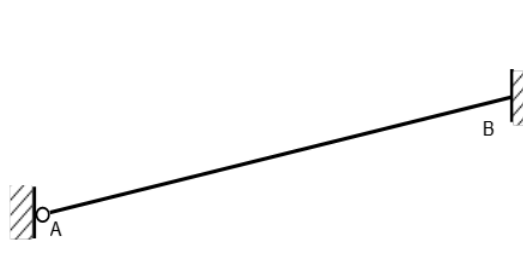$$

$$ m = K \ \theta $$

Figure 1. Unconnected element with fixed-fixed ends.

The corresponding member stiffness matrix is Equation 3:
where:
θ is the sectional strains vector; e, ϕ and β are member strains; T_m is the axial tension force; MAB_{zm} is the moment applied at joint A in z-axis; MBA_{zm} is the moment applied at joint B in z-axis; MAB_{ym} is the moment applied at joint A in y-axis; MBA_{ym} is the moment applied at joint B in y-axis; Q_m is the twisting moment in x-axis; VAB_{ym} is the normal shear force at joint A in y-axis; VBA_{ym} is the normal shear force at joint B in y-axis; VAB_{zm} is the normal shear force at joint A in z-axis; VBA_{zm} is the normal shear force at joint B in z-axis; L is the member length; E is the elastic modulus; G is the shear modulus; A is the cross-section area; I_z is the inertia moment in z-axis; I_y is the inertia moment in y-axis; and I_x is the torsion constant.

Unconnected element with the left end hinged, and the right end fixed

$$
\begin{bmatrix} T_m \\ MAB_{zm} \\ MBA_{zm} \\ MAB_{ym} \\ MBA_{ym} \\ Q_m \end{bmatrix} =
\begin{bmatrix}
\frac{EA}{L} & 0 & 0 & 0 & 0 & 0 \\
0 & 0 & 0 & 0 & 0 & 0 \\
0 & 0 & \frac{3EI_z}{L} & 0 & 0 & 0 \\
0 & 0 & 0 & 0 & 0 & 0 \\
0 & 0 & 0 & 0 & \frac{3EI_y}{L} & 0 \\
0 & 0 & 0 & 0 & 0 & 0
\end{bmatrix}
\begin{bmatrix} e \\ \phi AB_z \\ \phi BA_z \\ \phi AB_y \\ \phi BA_y \\ \beta \end{bmatrix} \quad (4)
$$

Figure 2. Unconnected element with hinged and fixed ends.

The modified member stiffness matrix is presented in Equation 4 (Figure 2).

Unconnected element with right end hinged, and left end fixed
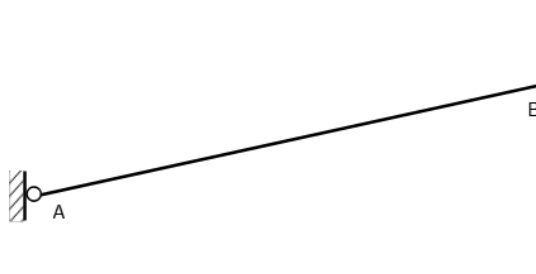
$$\begin{bmatrix} T_m \\ MAB_{zm} \\ MBA_{zm} \\ MAB_{ym} \\ MBA_{ym} \\ Q_m \end{bmatrix} = \begin{bmatrix} \frac{EA}{L} & 0 & 0 & 0 & 0 & 0 \\ 0 & \frac{3EI_z}{L} & 0 & 0 & 0 & 0 \\ 0 & 0 & 0 & 0 & 0 & 0 \\ 0 & 0 & 0 & \frac{3EI_y}{L} & 0 & 0 \\ 0 & 0 & 0 & 0 & 0 & 0 \\ 0 & 0 & 0 & 0 & 0 & 0 \end{bmatrix} \begin{bmatrix} e \\ \phi AB_z \\ \phi BA_z \\ \phi AB_y \\ \phi BA_y \\ \beta \end{bmatrix} \quad (5)$$

Figure 3. Unconnected element with fixed and hinged end.

The member stiffness matrix in this case is Equation 5 (Figure 3).

Unconnected element with hinged-hinged ends

$$\begin{bmatrix} T_m \\ MAB_{zm} \\ MBA_{zm} \\ MAB_{ym} \\ MBA_{ym} \\ Q_m \end{bmatrix} = \begin{bmatrix} \frac{EA}{L} & 0 & 0 & 0 & 0 & 0 \\ 0 & 0 & 0 & 0 & 0 & 0 \\ 0 & 0 & 0 & 0 & 0 & 0 \\ 0 & 0 & 0 & 0 & 0 & 0 \\ 0 & 0 & 0 & 0 & 0 & 0 \\ 0 & 0 & 0 & 0 & 0 & 0 \end{bmatrix} \begin{bmatrix} e \\ \phi AB_z \\ \phi BA_z \\ \phi AB_y \\ \phi BA_y \\ \beta \end{bmatrix} \quad (6)$$

Figure 4. Unconnected element with hinged-hinged ends.

The member stiffness matrix in this case is Equation 6 (Figure 4).

In the incremental analysis the following basic criteria were adopted:

• When the formation of the plastic hinge occurs due to one of the working moments in the section, we assume that it has formed in all directions of the section in the case of bending with single or double reinforcement and uniaxial bending;

• During the formation of the plastic hinge, there are two interaction situations between the normal stress and the moments: 1) taking normal stress into account, testing the variation in its numerical value at each phase of the formation of plastic hinges (this is the method used here); or 2) not considering its numerical value, removing it from the member stiffness matrix together with the moments;

• In the verification of the plastic rotation capacity, the total plastic rotation of the section was adopted as a limit value, without deducting the elastic rotation. The formulation is compatible with NBR 6118 (ABNT, 2014). Other methods can be seen in Orozco (2015);

• The method in this article is simpler in relation to the method proposed in Salihovic and Ademovi (2017) applied in a space frames analysis.

Uniaxial bending

Based on the formulation Mello (2003) proposed, the equilibrium equations of sections with reinforcement will be presented in this section with a focus on NBR 6118 (ABNT, 2014). The reinforcement arrangement is presented together with the applied axial loads and moment in Figure 5.

The equilibrium relations have the following definitions:

$$A_{cc} = b \cdot u; \quad q = b \cdot \sigma_{cd}; \quad R_c = A_{cc} \cdot \sigma_{cd} = q \cdot u; \quad \alpha = \frac{u}{h}; \qquad (7a)$$

$$a_1 = a_0 + z; \quad \alpha_0 = \frac{a_0}{h}; \quad \alpha_1 = \frac{a_1}{h}; \quad K_z = \frac{z}{h}; \quad z = a_1 - a_0 \qquad (7b)$$

where:

A_{cc} is the compressed concrete area; b and h are the cross-section dimensions; $\sigma_{cd} = 0.85 f_{cd}$ (calculated stress of the reinforced concrete); u is the cross-section compressed area; q is the partial uniform load in a

rigid beam of height h; R_c is the compression stresses resultant; α is the relative abscissa of the compressed concrete block; z is the lever arm; and a_0 is the cover of the section.

$$N_d = q \cdot u \text{ with } 0 < u \leq h; M_d = \frac{1}{2} q(h - u)u; \tag{8a}$$

$$v_d = \frac{N_d}{qh} = Fv(\alpha) = \alpha; \mu_d = \frac{8M_d}{qh^2} = F\mu(\alpha) = 4(1 - \alpha)\alpha \tag{8b}$$

where:

N_d is the calculated applied axial load; M_d is the calculated applied moment; v_d is the calculated relative normal working stress; and μ_d is the calculated relative bending working stress.

When requests (v_d and μ_d) occur outside the statically permissible region, the use of reinforcements is necessary, with more details in Mello (2003). In the arrangement of reinforcements shown in Figure 5, the forces R_n actuate for the equilibrium of N_d, and the binary in z of R_m, for the equilibrium of M_d.

The conditions of equilibrium will be:

$$\sum F_v = 0; 2R_n = N_d - q \cdot u; \sum M = 0; R_m = M_d - \frac{1}{2} q(h - u)u \tag{9}$$

In the dimensionless form:

$$R_n = \frac{1}{2}qh[v_d - F_v(\alpha)]; R_m = \frac{1}{2}qh\frac{[\mu_d - F_u(\alpha)]}{4K_z} \tag{10}$$

The terms applied in the computer program developed in Python Software Foundation (2021), version 3.8, are:

$$e_{0d} = v_d + \frac{\mu_d}{4K_z}; e_{1d} = v_d - \frac{\mu_d}{4K_z}; Fe_0(\alpha) = \alpha + \frac{4(1-\alpha)\alpha}{4K_z} = \frac{(2\alpha_1 - \alpha)\alpha}{K_z}; \tag{11a}$$

$$Fe_1(\alpha) = \alpha - \frac{4(1-\alpha)\alpha}{4K_z} = \frac{(\alpha - 2\alpha_0)\alpha}{K_z} \tag{11b}$$

where:

e_{0d} and e_{1d} are equivalent actions; Fe_0 and Fe_1 are equivalent resistance functions.
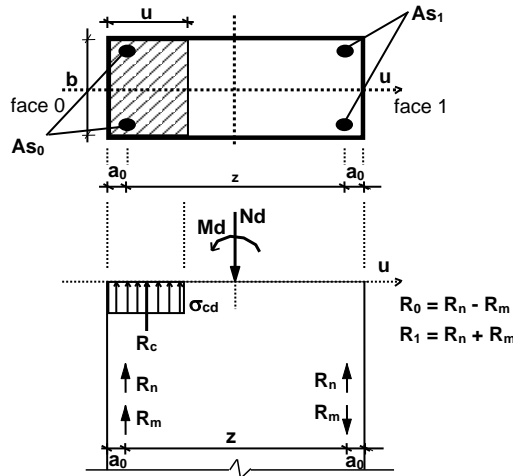

Figure 5. Statics of the reinforced section.

The expressions of Equation 11a-b can be seen graphically with more details in Mello (2003).

The resultant forces of Figure 5 are represented in relation to the terms R_0 and R_1 as

$$R_0 = \frac{1}{2}qh[e_{0d} - Fe_0(\alpha)] = R_n + R_m; R_1 = \frac{1}{2}qh[e_{1d} - Fe_1(\alpha)] = R_n - R_m \tag{12}$$

According to what has been described by Mello (2003), the properties of R_0 and R_1 cancel each other if:

$$e_{0d} = Fe_0(\alpha); e_{1d} = Fe_1(\alpha) \tag{13}$$

The solution of the two cases of Equation 13 leads to the solutions of second-degree equations for 'α', as follows:

$$\alpha^2 - 2\alpha_1\alpha + K_z e_{0d} = 0; \alpha^2 - 2\alpha_0\alpha - K_z e_{1d} = 0 \tag{14}$$

The solutions are:

$$\alpha_{R0} = \alpha_1 \left(1 \pm \sqrt{1 - \frac{e_{0d}}{Fe_0(\alpha_1)}}\right); \; \alpha_{R1} = \alpha_0 \left(1 \pm \sqrt{1 - \frac{e_{1d}}{Fe_1(\alpha_0)}}\right) \qquad (15)$$

Due to the many possible values for α, the reading of the evaluations made by Mello (2003) is recommended.

Neutral axis

The mechanisms of plastic collapse for the calculation of the cross-section curvature and the deformations in the reinforcements can be best studied in Mello (2003). The equivalent rectangular diagram from NBR 6118 (ABNT, 2014) is used for reinforced concrete with classes up to C50 (50 MPa) in this study.

The position of the neutral axis (α_x) is necessary to define the strain state of the evaluated element's cross-section. Then,

$$u = 0.8x; \; \alpha = 0.8\alpha_x \qquad (16)$$

where:

x is the position of the neutral axis; and α_x is the relative position of the neutral axis ($\alpha_x = \frac{x}{h}$).

According to the variation of the neutral axis α_x, the actions and the equivalent resistances are determined in R_0 and R_1. The mechanisms defined according to the position of the neutral axis belong to the domain of $\alpha \in [-\infty; +\infty]$.

The values defined by the Mello (2003) model for the neutral axis are:

- if $\alpha_x \geq \frac{5}{4}$, then $\alpha = 1$ (uniformly compressed section) is adopted; if $0 < \alpha_x \leq \frac{5}{4}$, then $\alpha = \frac{5}{4}$ (partially compressed section); if $\alpha_x \leq 0$ then $\alpha = 0$ (resistance to traction is neglected) is adopted.

In the computer program, the inferior limit range 'l' and the superior 'r', intervals of $\alpha_{xl} \leq \alpha_x \leq \alpha_{xr}$ were adopted, according to the algorithm criteria in Figure 1. Table 1 is part of the FOB, FNC and FSA routines of Figure 7.

Table 1. Interval definition algorithm of α_x.

Algorithm 1	If not, then:
1. If $e_{0d} >= 0$ and $e_{0d} \leq Fe_0(\alpha_1)$, then:	Choose the α_{R1} of negative sign ($-$) of Equation 15
If $e_{0d} >= 1$, then:	Select $\alpha_{x3} = \frac{5}{4}\alpha_{R1}$; $ct2 = 1$ (control parameter)
Choose one of α_{R0} from Equation 15.	The intervals that have been tested are:
If not, then:	3. If $e_{0d} >= 0$, then:
Choose the α_{R0} of negative sign ($-$) of the Equation 15.	$\alpha_{xl0} = \alpha_0$; $\alpha_{xr0} = +\infty$
Select $\alpha_{x2} = \frac{5}{4}\alpha_{R0}$; $ct1 = 1$ (control parameter)	If not, then:
2. If $e_{1d} \geq Fe_1(\alpha_0)$ and $e_{1d} \leq 1$, then:	$\alpha_{xl0} = -\infty$; $\alpha_{xr0} = \alpha_0$
If $e_{1d} \leq 0$	4. If $e_{1d} >= 0$, then:
Choose one of α_{R1} from Equation 15	$\alpha_{xl1} = \alpha_1$; $\alpha_{xr1} = +\infty$
	If not, then:
	$\alpha_{xl1} = -\infty$; $\alpha_{xr1} = 0.98\alpha_0$

Source: The authors.

Deformation mechanism 1

The position of the neutral relative axis α_x is in the domain $\alpha_x \in [1; +\infty]$. The shortening of the concrete will be defined by the value of $\varepsilon_p = 2 \, mm/m$. The position of α_p will be equal to 3/7; the deformations in the reinforcing bars (rebars) and Curvature K_1 are defined in Mello (2003).

Deformation mechanism 2

The position of the neutral relative axis α_x is in the domain $\alpha_x \in [(7/27)\alpha_1; 1]$. It includes the domains of limit-stage 3 to 4 of NBR 6118 (ABNT, 2014), and, depending on the reinforcement's arrangement, a small domain section 2, according to Mello (2003). The hypotheses are bending with $\alpha_p = 0$ and $\varepsilon_p = \varepsilon_{c0} = 3.5 \, mm/m = constant$. The inferior limit of α_x is obtained with the proviso that the relative elongation does not exceed 10 mm/m. Then, $\alpha_x = (7/27)\alpha_1$.

Deformation mechanism 3

The position of the neutral relative axis α_x is in the domain $\alpha_x \in [-\infty; (7/27)\alpha_1]$. It includes the domains of last limit-stages 1 and 2 of NBR 6118 (ABNT, 2014), according to Mello (2003). The hypotheses have $\alpha_p = \alpha_1$ and $\varepsilon_p = \varepsilon_{s1} = -10 \, mm/m$. The inferior limit of α_x is obtained with the proviso that the relative elongation does not exceed 10 mm/m.

Relative stress-strain diagram of the steel

The criteria of steel deformation for the last limit stage follows the NBR 6118 (ABNT, 2014), according to calculated deformation (ε_s).

The calculated strain is represented as:

$$\varepsilon_{yd} = \frac{f_{yd}}{E_s} \tag{17}$$

• if $\varepsilon_s < \varepsilon_{yd}$ then $\sigma_s = \varepsilon_s E_s$ is adopted; if $\varepsilon_s \geq \varepsilon_{yd}$ then $\sigma_s = f_{yd}$ is adopted with the deformation sign ε_s.

According to Mello (2003) the criteria used in the computer program depend on K_y, which is defined as:

$$K_{yi} = \frac{\sigma_{si}}{f_{yd}} = \frac{\varepsilon_{si}}{\varepsilon_{yd}} \text{ with } i \in [0;1] \tag{18}$$

• Conditions:

1) if $|\varepsilon_{si}|/\varepsilon_{yd} < 1$ then $K_y = \varepsilon_{si}/\varepsilon_{yd}$ is adopted; 2) if $|\varepsilon_{si}|/\varepsilon_{yd} \geq 1$ then $K_y = \pm 1$ is adopted.

where:

E_s is longitudinal elastic modulus of steel; f_{yd} is the calculated stress; and ε_{yd} is the calculated strain.

Reinforcements mechanical ratio

The reinforcements obtained follow the criteria of resistance conditions, according to Equation 19. That means that actuating forces R_0 and R_1 cannot be greater than the structure's resistance capacity.

$$A_{s0} \cdot \sigma_{s0} \geq R_0 ; A_{s1} \cdot \sigma_{s1} \geq R_1 \tag{19}$$

With

$$\sigma_{s0} = \frac{f_{yd0}}{f_{cd}}; \sigma_{s1} = \frac{f_{yd1}}{f_{cd}}; T_0 = A_{s0} \cdot \sigma_{s0}; T_1 = A_{s1} \cdot \sigma_{s1} \tag{20}$$

where:

σ_{s0} and σ_{s1} are the applied stresses in the positions '0' and '1' of Figure 5; A_{s0} and A_{s1} are the reinforcements obtained due to the applied loads; R_0 and R_1 are the applied forces in the section; and T_0 and T_1 are the resistance equivalent forces of the section.

By replacing R_0 and R_1 in Equation 19, with R_0 and R_1 from Equation 12 divided by qh, the following is obtained:

$$\frac{A_{s0}}{bh} \frac{f_{yd0}}{f_{cd}} K_{y0} \geq \frac{0.85}{2} [e_{0d} - Fe_0(\alpha)]; \frac{A_{s1}}{bh} \frac{f_{yd1}}{f_{cd}} K_{y1} \geq \frac{0.85}{2} [e_{1d} - Fe_1(\alpha)] \tag{21}$$

By defining geometric (ρ_i) and mechanical (ω_i) ratios as

$$\rho_i = \frac{A_{si}}{bh} \text{ with } i \in [0;1]; \omega_i = \rho_i \frac{f_{ydi}}{f_{cd}} \tag{22}$$

and replacing the terms in Equation 21, the following is obtained:

$$\omega_0 K_{y0} \geq \frac{0.85}{2} [e_{0d} - Fe_0(\alpha)]; \omega_1 K_{y1} \geq \frac{0.85}{2} [e_{1d} - Fe_1(\alpha)] \tag{23}$$

Adopting the proposal according to Mello (2003) where by:

$$Fs_0 \geq \frac{2K_{y0}}{0.85}; Fs_1 \geq \frac{2K_{y1}}{0.85} \tag{24}$$

Then:

$$\omega_0 Fs_0 + Fe_0(\alpha) \geq e_{0d}; \omega_1 Fs_1 + Fe_1(\alpha) \geq e_{1d} \tag{25}$$

Equation 25 are used as a base to obtain the plastic collapse load factor.

Plastic collapse load factor

The formulation involves the bending beam theory for singly or doubly reinforced beams, and columns with uniaxial or biaxial bending, proposed by Mello (2003) and adapted to NBR 6118 (ABNT, 2014) in this study. The part involving Equation 26 to 30 is distinct from the model proposed by (Mello, 2003).

Taking Equation 11a-b in which the terms of the applied actions receive a load factor γ_i, then:

$$\gamma_0 e_{0d} = \gamma_0 \left(v_d + \frac{\mu_d}{4K_z} \right); \gamma_1 e_{1d} = \gamma_1 \left(v_d - \frac{\mu_d}{4K_z} \right) \tag{26}$$

Replacing terms in Equation 26 with those from 25, it is possible to obtain the terms for the load factors in the section.

$$\omega_0 Fs_0 + Fe_0(\alpha) \geq \gamma_0 e_{0d}; \omega_1 Fs_1 + Fe_1(\alpha) \geq \gamma_1 e_{1d} \tag{27}$$

Then:

$$\gamma_0 \leq \frac{\omega_0 Fs_0 + Fe_0(\alpha)}{e_{0d}}; \gamma_1 \leq \frac{\omega_1 Fs_1 + Fe_1(\alpha)}{e_{1d}} \tag{28}$$

The section load factor is the least value of the values obtained:

$$\gamma^{seção} = min\,(\gamma_0; \gamma_1) \tag{29}$$

The load factor in each increment is obtained with the least factor for all the sections analyzed.

$$\gamma^j = min\,(\gamma^{seção1}; \gamma^{seção2}; \cdots; \gamma^{seçãon}) \tag{30}$$

where:
j is the number of increments in the analysis; and n is the number of sections analyzed in the structure.

The load factor involves the axial and bending moment efforts in y-axis and z-axis directions of the cross-section for singly or doubly reinforced beams and columns with uniaxial bending. In the case of columns with biaxial bending, the biaxial bending method is used.

For the obtention of the collapse load factor (γ^j) the following possibilities were considered based on information provided by Table 1. Table 2 is part of the FOB, FNC and FSA routines of Figure 7.

Table 2. Tests of γ^j.

Algorithm 2
1st Phase: test to verify if a minimum reinforcement is necessary.
1. Calculation of $v_s = 4v_d(1 - v_d)$ with v_d (Equation 8b) and μ_d (Equation 8b).
If $\mu_d \leq vs$, then:
Adopt minimum reinforcement.
$\gamma_0 = +\infty$ and $\gamma_1 = +\infty$
Exit
2nd Phase: tests for $\gamma_0 = \gamma_1$
1. Adopt $\alpha_{xl} = -\infty; \alpha_{xr} = +\infty$
2. Use ω_{s0} and ω_{s1} = arbitrated reinforcements (doubly reinforced section)
3. Obtain by root isolation the α_x for $\gamma_0 = \gamma_1$
4. To α_x obtain $R_0; R_1; T_0 = R_0 \times \sigma_{s0}; T_1 = R_1 \times \sigma_{s1}; \sigma_{s0}; \sigma_{s1}$
5. Check parity:
If $T_0 \geq 0$ and $T_1 \geq 0$ and $\gamma_0 \geq 0$ and $\gamma_1 \geq 0$, then:
γ_0 and γ_1 are possible solutions.
Exit
If not, then:
If $ct1 = 1$ and $ct2 = 1$, then:
$\omega_{s0} = 0$ and $\omega_{s1} = 0$ (section without reinforcement)
If $\alpha_{x2} \geq \alpha_{x3}$
$\alpha_{xl} = \alpha_{x2}; \alpha_{xr} = \alpha_{x3}$
If not, then:
γ_0 and γ_1 are possible solutions
$\alpha_x = \alpha_{xm}$
Exit
If not, then:
$test = test + 1$
If $test = 1$, then:
Use $\omega_{s0} = 0$ and ω_{s1} = arbitrated reinforcement
Obtain the minimum root (α_{xm}) in the intervals:
a) $\alpha_{xl} = \alpha_{xl1}; \alpha_{xr} = \alpha_{xr1}$
b) $\alpha_{xl} = \alpha_{xl0}; \alpha_{xr} = \alpha_{xr0}$
To α_{xm} obtain $R_0; R_1; T_0 = R_0 \times \sigma_{s0}; T_1 = R_1 \times \sigma_{s1}; \sigma_{s0}; \sigma_{s1}$
Check parity:
If $T_0 \geq 0$ and $T_1 \geq 0$ and $\gamma_0 \geq 0$ and $\gamma_1 \geq 0$, then:
γ_0 and γ_1 are possible solutions
$\alpha_x = \alpha_{xm}$
Exit
If not, then:
$test = test + 1$
If $test = 2$, then:
Use ω_{s0} = arbitrated reinforcement and $\omega_{s1} = 0$
Obtain the minimum root (α_{xm}) in the intervals:
a) $\alpha_{xl} = \alpha_{xl1}; \alpha_{xr} = \alpha_{xr1}$
b) $\alpha_{xl} = \alpha_{xl0}; \alpha_{xr} = \alpha_{xr0}$
To α_{xm} obtain $R_0; R_1; T_0 = R_0 \times \sigma_{s0}; T_1 = R_1 \times \sigma_{s1}; \sigma_{s0}; \sigma_{s1}$
Check parity:

Algorithm 2 (continued)
$\alpha_{xl} = \alpha_{x3}; \alpha_{xr} = \alpha_{x2}$
Repeat step 5.
If $ct1 = 1$ and $ct2 = 0$, then:
Use $\omega_{s0} = 0$ and ω_{s1} = arbitrated value (simple bending section)
$\alpha_{xl} = \alpha_{xl0}; \alpha_{xr} = \alpha_{x2}$
Repeat steps 3. to 5.
If $ct1 = 0$ and $ct2 = 1$, then:
ω_{s0} = arbitrated value and $\omega_{s1} = 0$ (simple bending section)
$\alpha_{xl} = \alpha_{xl1}; \alpha_{xr} = \alpha_{x3}$
Repeat steps 3 to 5
3rd Phase: tests to $\gamma_0 \neq \gamma_1$
1. test = 0
2. While $test \leq 3$, do:
If $test = 0$, then:
Use ω_{s0} and ω_{s1} = arbitrated reinforcement
Obtain the minimum root (α_{xm}) in the intervals:
$\alpha_{xl} = \alpha_{xl1}; \alpha_{xr} = \alpha_{xr1}$
a) $\alpha_{xl} = \alpha_{xl0}; \alpha_{xr} = \alpha_{xr0}$
To α_{xm} obtain $R_0; R_1; T_0 = R_0 \times \sigma_{s0}; T_1 = R_1 \times \sigma_{s1}; \sigma_{s0}; \sigma_{s1}$
Check parity:
If $T_0 \geq 0$ and $T_1 \geq 0$ and $\gamma_0 \geq 0$ and $\gamma_1 \geq 0$, then:
If $T_0 \geq 0$ and $T_1 \geq 0$ and $\gamma_0 \geq 0$ and $\gamma_1 \geq 0$, then:
γ_0 and γ_1 are possible solutions
$\alpha_x = \alpha_{xm}$
Exit
If not, then:
$test = test + 1$
If $test = 3$, then:
Use $\omega_{s0} = 0$ and $\omega_{s1} = 0$
Obtain the minimum root (α_{xm}) in the intervals:
a) $\alpha_{xl} = \alpha_{xl1}; \alpha_{xr} = \alpha_{xr1}$
b) $\alpha_{xl} = \alpha_{xl0}; \alpha_{xr} = \alpha_{xr0}$
To α_{xm} obtain $R_0; R_1; T_0 = R_0 \times \sigma_{s0}; T_1 = R_1 \times \sigma_{s1}; \sigma_{s0}; \sigma_{s1}$
Check parity:
If $T_0 \geq 0$ and $T_1 \geq 0$ and $\gamma_0 \geq 0$ and $\gamma_1 \geq 0$, then:
γ_0 and γ_1 are possible solutions
$\alpha_x = \alpha_{xm}$
Exit
If not, then:
$test = test + 1$
If $test > 3$, then:
γ_0 and γ_1 we're not found with these criteria
Stop program.
4th Phase:
1. To α_x obtain $R_0; R_1; T_0 = R_0 \times \sigma_{s0}; T_1 = R_1 \times \sigma_{s1}; \sigma_{s0}; \sigma_{s1};$
$\gamma_0; \gamma_1$
2. Check parity:
If $T_0 \geq 0$ and $T_1 \geq 0$ and $\gamma_0 \geq 0$ and $\gamma_1 \geq 0$
Print results

Source: The authors.

The biaxial bending model will be the same as that presented by Mello (2003), using an interpolation function and reinforcement arrangements as shown in Figure 6 which, however, are only illustrative. Obtaining the reinforcement is one of the objectives of the proposed model.

The angle θ is the result of the relations of the relative eccentricities ξ_b and ξ_h, taking the direction h as a reference.

$$tan(\theta) = \frac{\xi_b}{\xi_h} \text{ with } 0 \leq \theta \leq \pi/2 \tag{31}$$

With

$$\xi_b = \frac{e_{1z}}{b}; \; \xi_h = \frac{e_{1y}}{h} \tag{32}$$

where:

ξ_b and ξ_h are the relative eccentricities; e_{1z} and e_{1y} are the initial biaxial bending eccentricities of the 1st order.

The angle φ comes from geometric properties of the section so that

$$tan(\varphi) = \frac{b}{h} \tag{33}$$

The function of interpolation $f(\theta)$ for the stress σ_{cd} has the following description:

- If the angle θ ≤ φ

$$f(\theta) = 0.85 - 0.05 \frac{h}{b} tan(\theta); \; f(t) = 0.85 - 0.05 \left(\frac{h}{b}\right)\frac{\xi_b}{\xi_h} \tag{34}$$

- If the angle θ > φ

$$f(\theta) = 0.85 - 0.05 \frac{b}{h} tan(\theta); \; f(t) = 0.85 - 0.05 \left(\frac{b}{h}\right)\frac{\xi_h}{\xi_b} \tag{35}$$

With

$$t = sin^2(\theta) \text{ with } 0 \leq t \leq 1 \tag{36}$$

Biaxial bending

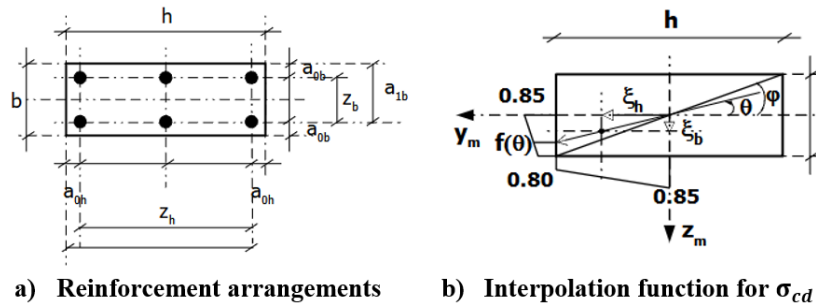a) **Reinforcement arrangements**   b) **Interpolation function for σ_{cd}**

Figure 6. Biaxial bending model.

The applied stress in the angle θ will be calculated in the following manner:

$$\sigma_{cdt} = f(t)\sigma_{cd} \tag{37}$$

Using the relations of Equation 8a-b and 11a-b expressed expressed for the case of biaxial bending:

$$v_{dt} = \frac{N_d}{bh\sigma_{cdt}} = \frac{N_d}{q_t h} = \frac{N_d}{A\sigma_{cdt}} \tag{38}$$

where:

v_{dt} is the calculated relative normal working stress.

The equivalent actions are presented by Mello (2003) as follows:

- Direction h

$$e_{0dh} = \left[1 + 2\left(\frac{e}{z}\right)_h\right]v_{dt}; \; e_{1dh} = \left[1 - 2\left(\frac{e}{z}\right)_h\right]v_{dt} \tag{39}$$

- Direction b

$$e_{0db} = \left[1 + 2\left(\frac{e}{z}\right)_b\right]v_{dt}; \; e_{1db} = \left[1 - 2\left(\frac{e}{z}\right)_b\right]v_{dt} \tag{40}$$

In function $\left(\frac{e}{z}\right)_t$, in the following manner:

$$\left(\frac{e}{z}\right)_t = (1 - t)\left(\frac{e_{1y}}{z}\right)_h + t\left(\frac{e_{1z}}{z}\right)_b \tag{41}$$

$$e_{0dt} = \left[1 + 2\left(\frac{e}{z}\right)_t\right]\nu_{dt}; e_{1dt} = \left[1 - 2\left(\frac{e}{z}\right)_t\right]\nu_{dt} \tag{42}$$

The working moments follow the same procedures adopted for axial stresses, as

$$\mu_{dh} = 8\nu_{dt}\left(\frac{e_{1y}}{h}\right); \mu_{db} = 8\nu_{dt}\left(\frac{e_{1z}}{b}\right) \tag{43}$$

The interpolation formula will be based on t:

$$\mu_t = (1 - t)\mu_{dh} + t\mu_{db} \tag{44}$$

where:

μ_{dh} and μ_{db} are the relative applied stresses in directions y and z.

Equation 41, 42, 43, and 44 are used in the program developed, along with the other relations of Equation 31 to 38.

The other relations used for the formulation, based on Figure 3, are the following:

$$K_{zh} = \frac{z_h}{h}; K_{zb} = \frac{z_b}{b}; K_{zt} = (1 - t)K_{zh} + t K_{zb} \tag{45}$$

$$q_t = b\sigma_{cdt}; \alpha_{0y} = \frac{a_{0h}}{h}; \alpha_{1y} = \frac{a_{1h}}{h} \tag{46a}$$

$$\alpha_{0z} = \frac{a_{0b}}{b}; \alpha_{1z} = \frac{a_{1b}}{b} \tag{46b}$$

$$\alpha_{0t} = (1 - t)\alpha_{0y} + t \alpha_{0z}; \alpha_{1t} = (1 - t)\alpha_{1y} + t \alpha_{1z} \tag{46c}$$

The procedures follow the same logic of uniaxial bending, considering the use of the interpolation function with 't' in order to direct the angle θ; for more details see Mello (2003).

The criteria of NBR 6118 (ABNT, 2014) in relation to the rules of uniaxial bending, and biaxial bending, in its items 11.3.3.4.3 (minimum bending moment) and 15.8 (isolated elements analysis), were implemented to calculate, if necessary, the total moments for columns with slenderness ratio $\lambda \leq 90$. Two approximate standard-column methods (standard-column method with approximate rigidity and standard-column method with approximate curvature) were used. The values of the two directions of cross-section were obtained and the one with the highest total value of moments ($M_{d,tot}$) was chosen. Other similar studies are those of Sfakianakis (2002), and Al-Ansari and Afzal (2020).

Schematic diagram of the method

The summary of procedures for the presented method are described in Figure 7, 8 and 9.

The input data (INPUT in Figure 7) is as follows: NN is total number of nodes; NE is the total number of elements or bars; NDF is the number of degrees of freedom per node; MS is the semi-bandwidth of the total stiffness matrix; NNE is the number of nodes per element; NL is the total number of nodal loads; NC is the total number of boundary conditions; ITC is the monitoring node; TG is the graphic type; G_c is the concrete reduction factor; G_s is the steel reduction factor; GF is the loads magnification factor; ν is the Poisson's ratio; E_c is the modulus of elasticity of concrete; E_s is the modulus of elasticity of steel; ENM is the plastic hinge type; X, Y and Z are the nodal coordinate vectors; CON is the element connectivities array; IRZ is the element rigidity conditions vector; b is the cross-section width; db is the effective width; h is the cross-section overall depth; dh is the effective depth; TA is the steel strength type; fck is the concrete strength; fyk is the steel yield strength; AL is the applied loads vector; the cross-section properties are those seen in Figure 1 and Figure 5; ωs_1 and ωs_0 are the reinforcement rates; and T_b is the element type as in Figure 7.

Characterization of cases

The cases are related to the formulation presented to verify the importance of the design conception and the applicability of the formulation to obtain plastic collapse load factors, and their formation trajectory.

Case 1 is based on space frame data presented by Harrison (1973), with 3 elements and 4 discretized nodes, according to Figure 10.
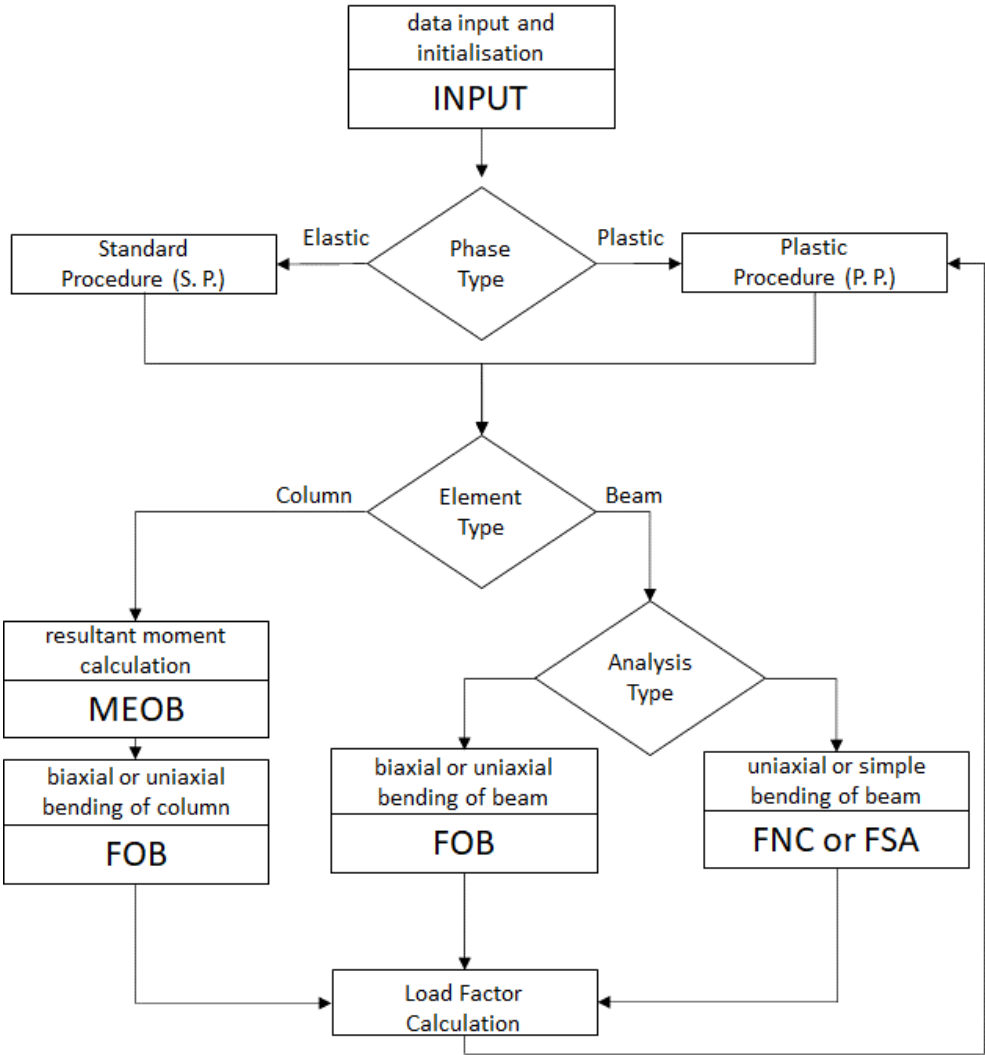
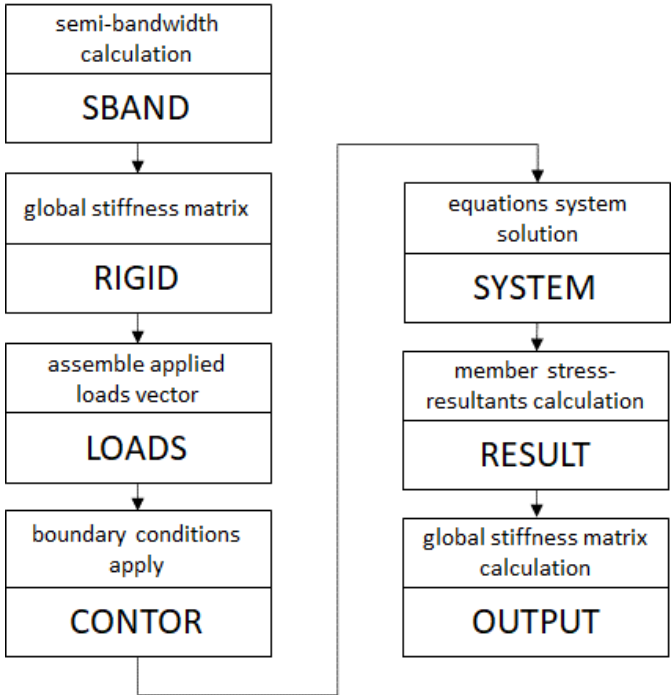**Figure 7.** General schematic diagram.

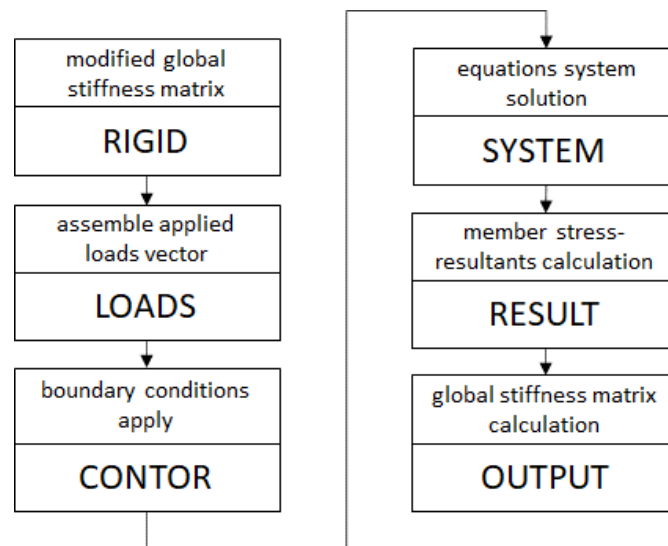**Figure 8.** Standard procedure (S. P.) schematic diagram.

Figure 9. Plastic procedure (P. P.) schematic diagram.

Properties of the space frame (SP):
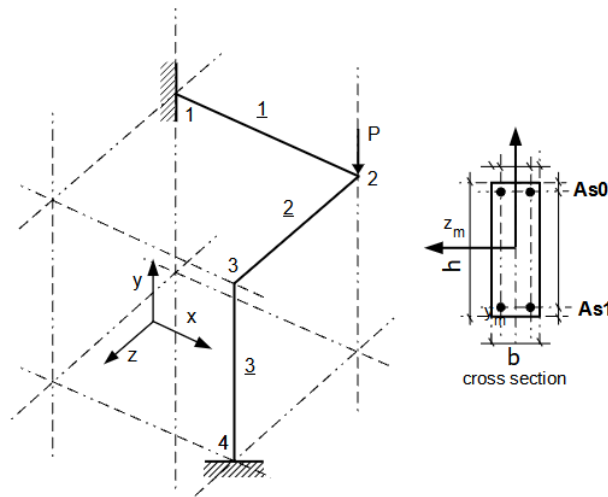
Figure 10. Space frame – Harrison.

Table 3. Coordinates of the space frame – Harrison.

Node	X	Y	Z
	(m)	(m)	(m)
1	0.000	12.000	0.000
2	12.000	12.000	0.000
3	12.000	12.000	12.000
4	12.000	0.000	12.000

Table 4. Physical characteristics of the space frame – Harrison

Elem.	Node I	Node F	$(kN\ m^{-2})$	$(kN\ m^{-2})$	v
1	1	2	E_s	F_{yk}	
			201.037×10^6	490.335×10^3	0.20
2	2	3			
			E_c	F_{ck}	L
3	3	4	31.57×10^6	19613.40	12 m

The terms of Table 4 have the following description: E_s is the modulus of elasticity of steel; E_c is the longitudinal modulus of elasticity of the concrete; $G_c = \frac{E_c}{2(1+v)}$ (shear modulus of elasticity of concrete); v is the Poisson's ratio; F_{yk} is the yield stress of steel; F_{ck} *is the* maximum stress of concrete; and L is the span length.

Table 5. Material properties of the space frame – Harrison.

Element	Cross-section
1,2 and 3	A = 0.18 m^2 b = 0.3 m and h = 0.6 m I_z = 5400.00 ×10^{-6} m^4 I_y = 1350.00 ×10^{-6} m^4 I_x = 3710.00 ×10^{-6} m^4

where:

A is the cross-section area; b is the width of the cross-section; h height of the cross-section; I_z is the moment of inertia in the z direction; I_y is the moment of inertia in the y direction; and I_x is the torsion constant.

Table 6. Applied loads of the space frame – Harrison.

Node	Dir	Value (kN)
2	F_y	-9.807

where:

F_y is the applied force in y direction.

Project conceptions were implemented in 2 (two) types that are described in Table 7.

Table 7. Project Conceptions – space frame – Harrison.

	Phar1					Phar2			
Elem.	$\omega s_1(\%)$	$\omega s_0(\%)$	T_b	$a_{0b} = a_{0h}$ (m)	Elem.	$\omega s_1(\%)$	$\omega s_0(\%)$	T_b	$a_{0b} = a_{0h}$ (m)
1	1.5	0.75	13	0.015	1	1.5	0.75	12	0.015
2	1.5	0.75	13	0.015	2	1.5	0.75	12	0.015
3	1.5	0.75	2	0.015	3	1.5	0.75	21	0.015

where:

The column (biaxial bending) - T_b = 2; the column (uniaxial bending) - T_b = 21; the singly reinforced beam - T_b = 11; the doubly reinforced beam (uniaxial bending) - T_b = 12; the doubly reinforced beam (biaxial bending) - T_b = 13; and ωs_1 and ωs_0 are the reinforcement rates.

Case 2 is based on the space frame with data provided by Gere and Weaver Jr. (1987), according to Figure 11.
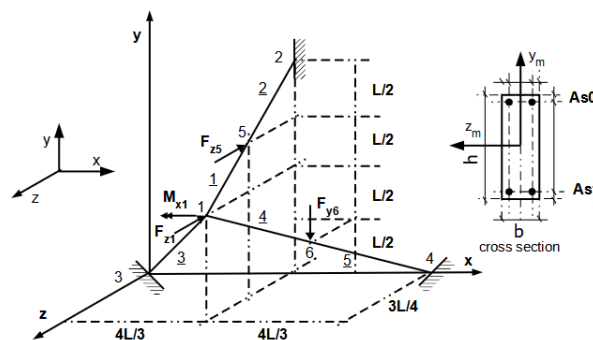
Figure 11. Space frame - Gere & Weaver.

Table 8. Coordinates of the space frame - Gere & Weaver.

Node	X	Y	Z
	(m)	*(m)*	*(m)*
1	4.000	3.000	2.250
2	4.000	6.000	0.000
3	0.000	0.000	0.000
4	8.000	0.000	0.000
5	4.000	4.500	1.125
6	6.000	1.500	1.125

The properties of the case are presented in Table 8 to Table 10.

Table 9. Physical characteristics of the space frame - Gere & Weaver.

Elem.	Node I	Node F	$(kN\ m^{-2})$	$(kN\ m^{-2})$	
1	1	5	E_s	F_{yk}	ν
2	5	2	201.037×10^6	490.335×10^3	0.2
3	3	1			
4	1	6	E_c	F_{ck}	L
5	6	4	31.57×10^6	19613.40	3 m

Table 10. Material properties of the space frame - Gere & Weaver.

Element (Elem.)	Cross-section
	$A = 0.08\ m^2$
	$b = 0.2\ m$ and $h = 0.4\ m$
1 a 5	$I_z = 1066.667 \times 10^{-6}\ m^4$
	$I_x = 732.800 \times 10^{-6}\ m^4$
	$I_y = 266.667 \times 10^{-6}\ m^4$

The applied loads are the following:

Table 11. Applied loads of the space frame - Gere & Weaver.

Node	$F_y(kN)$	$F_z(kN)$	$M_x(kN \cdot m)$
1	0.000	-22.2411	0.000
1	0.000	0.000	-16.6808
5	0.000	-22.2411	0.000
6	-22.2411	0.000	0.000

With $M_x = PL/4$ and $F_y = F_z = 22.2411$.

Project conceptions were implemented in 3 (three) types that are described in Table 12.

Table 12. Project Conceptions - space frame - Gere & Weaver.

	PGere&Weaver1					PGere&Weaver3			
Elem.	$\omega s_1(\%)$	$\omega s_0(\%)$	T_b	$a_{0b} = a_{0h}\ (m)$	Elem.	$\omega s_1(\%)$	$\omega s_0(\%)$	T_b	$a_{0b} = a_{0h}\ (m)$
1	1.5	0.75	12	0.015	1	1.5	0.75	12	0.020
2	1.5	0.75	12	0.015	2	1.5	0.75	12	0.020
3	1.5	0.75	12	0.015	3	1.5	0.75	12	0.020
4	1.5	0.75	12	0.015	4	1.5	0.75	12	0.020
5	1.5	0.75	12	0.015	5	1.5	0.75	12	0.020
				PGere&Weaver2					
Elem.	$\omega s_1(\%)$		$\omega s_0(\%)$		T_b			$a_{0b} = a_{0h}\ (m)$	
1	1.5		0.75		2			0.015	
2	1.5		0.75		2			0.015	
3	1.5		0.75		2			0.015	
4	1.5		0.75		2			0.015	
5	1.5		0.75		2			0.015	

Results and discussion

The results and discussion of the case studies 1 to 2 are presented in this section.

Case 1

The displacements and sectional efforts from the first elastic phase of the program were validated with SAP200 v.22 software of the first elastic phase as seen in Table 13 and Table 14.

Table 13. Displacements - space frame - Harrison.

	SAP2000 v.22					
Node	u_1	u_2	u_3	r_1	r_2	r_3
1	0	0	0	0	0	0
2	9.198e-8	-0.022169	-0.007638	-0.001947	0.000868	-0.002675
3	0.008046	-5.533e-6	-0.007640	-0.001375	0.000449	-0.001366
4	0	0	0	0	0	0

| The authors | | | | | |
Node	u_1	u_2	u_3	r_1	r_2	r_3
1	0	0	0	0	0	0
2	0.000000	-0.022129	-0.007634	-0.001945	0.000868	-0.002676
3	0.008048	-0.000006	-0.007636	-0.001374	0.000449	-0.001366
4	0	0	0	0	0	0

Table 14. Sectional Efforts - space frame - Harrison.

| SAP2000 v.22 | | | | | |
Elem.- Node	P	V_2	V_3	T	M_2	M_3
1-1	-0.044	0.718	7.187	7.5972	81.1294	-7.3918
1-2	0.044	-0.718	-7.187	-7.5972	5.1112	-1.2276
⋮	⋮	⋮	⋮	⋮	⋮	⋮
3-3	2.620	0.718	0.044	-1,7503	-5.1112	23.8462
3-4	-2.620	-0.718	-0.044	1.7503	4.5885	-15.2267
The authors					
Elem.- Node	P	V_2	V_3	T	M_2	M_3
1-1	-0.043822	0.718125	7.188849	7.593434	81.15150	-7.391445
1-2	0.043822	-0.718125	-7.188849	-7.593434	5.114685	-1.226050
⋮	⋮	⋮	⋮	⋮	⋮	⋮
3-3	2.618151	0.718125	0.043822	-1.751909	-5.114685	23.824372
3-4	-2.618151	-0.718125	-0.043822	1.751909	4.588826	-15.206878

The results of the studies are presented in Table 15 and Figure 12, with the formulations of the proposed method. The number of plastic elements varied in the project conceptions adopted, being 2 (two) elements for Phar1 and 3 (three) for Phar2. The quantity of hinges was 3 (three) for both conceptions. The hinge formation paths are shown in Table 15 and Figure 12. Both conceptions had a clear influence on the structure's resistance capacity, i.e., Phar1 with load factor 2.6643 shows that the dimensioning of doubly reinforced beams (biaxial bending) and of columns with biaxial bending is safer than Phar2 with load factor 1.9049, which has doubly reinforced beams (uniaxial bending) and columns with uniaxial bending. In this case, the coverings were the same. The most important factor for the variation in the collapse load factor was that node 2, at the third plastic hinge, obtained parity (see Table 2) with single reinforcement for Phar1 and double reinforcement for Phar2. The case where the three (3) elements are dimensioned as columns gives the same result as case Phar1. This is because the biaxial bending analyses for columns and beams are similar, except for the issue of equivalent columns eccentricities and moments. The rotation angle was verified and did not exceed the limits of NBR 6118 (ABNT, 2014). The results are as follows: Phar1 and Phar2 with $\theta_{máx} = 0.01144$ and $\theta_{lim} = 0.015$.

Table 15. Plastic hinges – space frame - Harrison.

Phar1 (u_{y1})					Phar2(u_{y2})				
Plastic Hinge	Element	Node	λ	Limit load (kN)	Plastic Hinge	Element	Node	λ	Limit load (kN)
1	2	3	0.9996		1	3	3	1.0007	
2	1	1	1.8930	2.6643	2	1	1	1.8940	1.9049
3	2	2	2.6643		3	2	2	1.9049	
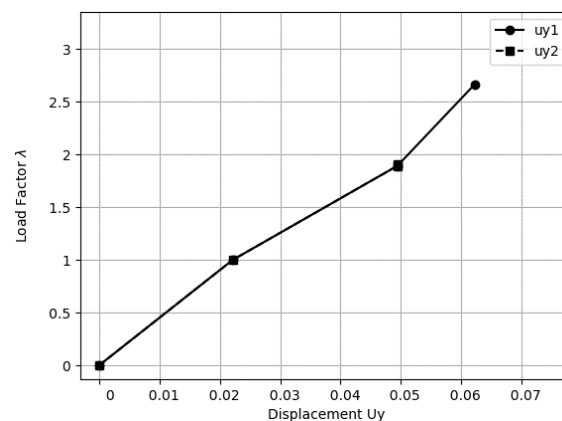
Figure 12. Applied load versus vertical displacement (u_y) - node 2 – space frame – Harrison.

Case 2

The displacements and sectional efforts from the first elastic phase of the program were validated with SAP200 v.22 (Computers & Structures, Inc, 2022)software of the first elastic phase as seen in Table 16 and 17.

Table 16. Displacements - space frame - Gere & Weaver.

Node	u_1	u_2	u_3	r_1	r_2	r_3
— SAP2000 v.22						
1	-0.000001094	-0.00002	-0.000082	-0.000552	0.000019	-0.000642
2	0	0	0	0	0	0
3	0	0	0	0	0	0
4	0	0	0	0	0	0
5	0.000235	-0.00026	-0.000383	0.000155	0.000233	-0.000022
6	-0.001299	-0.002001	0.000289	0.000043	0.000038	0.000209

Node	u_1	u_2	u_3	r_1	r_2	r_3
— The authors						
1	−0.000001	−0.000020	−0.000082	−0.000541	0.000019	−0.000640
2	0	0	0	0	0	0
3	0	0	0	0	0	0
4	0	0	0	0	0	0
5	0.000234	−0.000245	−0.000363	0.000166	0.000234	−0.000020
6	−0.001284	−0.001972	0.000277	0.000047	0.000037	0.000208

Table 17. Sectional Efforts - space frame - Gere & Weaver.

Elem.- Node	P	V_2	V_3	T	M_2	M_3
— SAP2000 v.22						
1-1	15.782	0.642	1.788	0.9872	-4.4799	12.0980
1-5	-15.782	0.642	-1.788	-0.9872	1.1281	13.3015
⋮	⋮	⋮	⋮	⋮	⋮	⋮
5-6	26.400	-4.661	-10.198	-0.2526	13.3794	-5.6971
5-4	-26.400	4.661	10.198	0.2526	14.5781	-7.0822

Elem.- Node	P	V_2	V_3	T	M_2	M_3
— The authors						
1-1	15.720715	0.523479	1.795657	0.984185	-4.490467	-12.219558
1-5	-15.720715	-0.523479	-1.795657	-0.984185	1.123611	13.201081
⋮	⋮	⋮	⋮	⋮	⋮	⋮
5-6	26.298606	-4.647485	-10.193192	-0.240746	13.370275	-5.655635
5-4	-26.298606	4.647485	10.193192	0.240746	14.573994	-7.085278

The results of the studies are presented in Table 18 and Figure 13. The number of elements with plastic hinges varied in the design conceptions adopted, being 2 (two) elements for PGere&Weaver1, 4 (four) for PGere&Weaver2, and 3 (three) for PGere&Weaver3. The hinge formation paths are shown in the table and the figure mentioned above. The design conceptions PGere&Weaver1 and PGere&Weaver3 are similar for doubly reinforced beams (uniaxial bending) but have distinct covers. The adoption of different cover thicknesses changes the load factor obtained because it interferes with the steel reinforcement. There was an increase in the load factor for PGere&Weaver3 in which the cover was greater than in PGere&Weaver1. PGere&Weaver2 has the column concept (biaxial bending). The design conception that permitted a higher load factor was PGere&Weaver2, with a load factor of 3.9989. The design concept as a column for this type of space frame was more appropriate in order to have a structure with better resistant capacity. This case of a space frame with its geometry can generate doubts about which would be the best way to execute it, i.e., as a beam or a column. However, the method presented makes it possible to evaluate which is the best execution process. It should be noted that mixed beam and column configurations were also tested, but load factors that met the parity criteria of Table 2 were not obtained. It is possible to use the option uniaxial bending for beam and/or column with minor quantities of reinforcement and less cost, but this method does not perform automatic optimization. The rotation angles were verified and did not exceed the limits of NBR 6118 (ABNT, 2014). The results were as follows: PGere&Weaver1 with $\theta_{máx} = 0.010878$ and $\theta_{lim} = 0.015$; PGere&Weaver2 with $\theta_{máx} = 0.013684$ and $\theta_{lim} = 0.015$; PGere&Weaver3 with $\theta_{máx} = 0.011931$ and $\theta_{lim} = 0.015$.

Table 18. Plastic hinges – space frame - Gere & Weaver.

PGere&Weaver1 (u_{y1})					PGere&Weaver3 (u_{y3})				
Plastic Hinge	Element	Node	λ	*Limit load* (*kN*)	Plastic Hinge	Element	Node	λ	*Limit load* (*kN*)
1	4	1	0.1321	0.7368	1	4	6	0.3965	
2	5	6	0.7368		2	1	1	0.5672	1.3994
					3	5	4	1.3994	
PGere&Weaver2 (u_{y2})									
Plastic Hinge		Element		Node		λ		*Limit load* (*kN*)	
1		5		6		0.9997		3.9989	
2		2		5		1.9994			
3		3		3		2.9991			
4		1		1		3.9989			
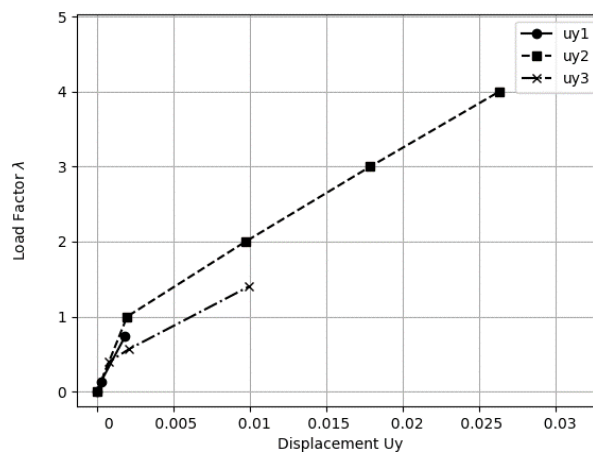
Figure 13. Applied load versus vertical displacement ($\boldsymbol{u_y}$) – node 6 - space frame - Gere & Weaver.

Conclusion

• Based on the results presented, designers should have comprehensive knowledge on structural safety to define a good design that makes projects safer in their implementation for several design conceptions. The better conception for a space frame – Harrison – should be dimensioned with doubly reinforced beam (biaxial bending) and column (biaxial bending). For the space frame conception of Gere & Weaver, it is better to use the column (biaxial bending). There is also the possibility of using the uniaxial bending option for beam and/or column with minor quantities of reinforcement and lower cost, but this method does not perform automatic optimization.

• Based on Melo's formulation, the present method is able to work with the design criteria of NBR 6118 (ABNT, 2014) to successfully obtain load factors, plastic collapse, and design according to the criteria of Vieira. It is a much simpler process for obtaining plastic hinges and their load factors without the use of methods with a reduced stiffness matrix or mesh refinement or plastic hinge length. The purpose of having a code for research development without the need for commercial software licenses has been achieved.

• The method suggested in this study is simpler than working with surface interaction for controlling the movement of a plastic force point over the yield surface or reduced stiffness matrix methods. Hence, it seems to be a viable technique for obtaining collapse load factors using elastic analysis and stiffness matrix's propriety changes for space frames.

• The present method shows that good safe designs for structural systems can be obtained using the project criteria of NBR 6118 (ABNT, 2014), according to the analysis carried out. It is necessary to test more examples for better conclusions, but the method presented in this study is an alternative technique for elastoplastic analysis.

Acknowledgements

References

Al-Ansari, M. S., & Afzal, M. S. (2020). Mathematical model for analysis of uniaxial and biaxial reinforced concrete columns. *Advances in Civil Engineering, 2020*, 8868481. DOI: https://doi.org/10.1155/2020/8868481

Associação Brasileira de Normas Técnicas [ABNT]. (2014). *NBR-6118: projeto de estruturas de concreto — procedimento.* Rio de Janeiro, RJ: ABNT.

Barham, W. S., Aref, A. J., & Dargush, G. F. (2005). Flexibility-based large increment method for analysis of elastic–perfectly plastic beam structures. *Computers & Structures*, *83*(28-30), 2453-2462. DOI: https://doi.org/https://doi.org/10.1016/j.compstruc.2005.03.037

Computers & Structures, Inc. (2022). *SAP2000. Structural analysis and design*. Retrieved from https://www.csiamerica.com/products/sap2000

Gere, J. M., & Weaver Jr., W. (1987). *Análise de estruturas reticulares.* São Paulo, SP: Guanabara.

Hanganu, A. D., Barbat, A. H., & Oñate, E. (1997). *Metodologia de evaluación del deterioro en estructuras de hormigón armado*. Barcelona, ES: Cimne.

Harrison, H. B. (1973). *Computer methods in structural analysis.* Englewood Cliffs, New Jersey: Prentice Hall.

Inel, M., & Ozmen, H. B. (2006). Effects of plastic hinge properties in nonlinear analysis of reinforced concrete buildings. *Engineering Structures, 28*(11), 1494-1502. DOI: https://doi.org/https://doi.org/10.1016/j.engstruct.2006.01.017

Mello, E. L. (2003). *Concreto armado: resistência limite à flexão composta normal e oblíqua.* Brasília, DF: Universidade de Brasília.

Orbison, J. G., McGuire, W., & Abel, J. F. (1982). Yield surface applications in nonlinear steel frame analysis. *Computer Methods in Applied Mechanics and Engineering*, *33*(1-3), 557-573. DOI: https://doi.org/https://doi.org/10.1016/0045-7825(82)90122-0

Orozco, C. E. (2015). Strain limits vs. reinforcement ratio limits – a collection of new and old formulas for the design of reinforced concrete sections. *Case Studies in Structural Engineering*, *4*, 1-13. DOI: https://doi.org/https://doi.org/10.1016/j.csse.2015.05.001

Patel, B. R. (2014). Progressive collapse analysis of rc buildings using linear static and linear dynamic method. *International Journal of Engineering Research & Technology, 3*(8), 1640-1644.

Python Software Foundation. (2021). *Python*. Retrieved from https://www.python.org

Salihovic, A., & Ademovic, N. (2017). Nonlinear analysis of reinforced concrete frame under lateral load. *Coupled Systems Mechanics*, *6*(4), 523-537. DOI: https://doi.org/https://doi.org/10.12989/csm.2017.6.4.523

Sfakianakis, M. G. (2002). Biaxial bending with axial force of reinforced, composite and repaired concrete sections of arbitrary shape by fiber model and computer graphics. *Advances in Engineering Software, 33*(4), 227-242. DOI: https://doi.org/10.1016/S0965-9978(02)00002-9

Silva, W. T. M. (2004). Análise elastoplastica de estruturas metálicas utilizando algorítmos de retorno radial. *Revista Internacional de Metodos Numericos para Calculo y Diseno en Ingenieria, 20*(3), 297-317.

Vieira, P. C. S., & Silva, W. T. M. (2013). Análise elastoplástica de estruturas aporticadas com superfícies de interação obtidas por regressão linear múltipla. *Revista Internacional de Métodos Numéricos para Cálculo y Diseño en Ingeniería, 29*(3), 175-187. DOI: https://doi.org/10.1016/j.rimni.2012.12.001